H-infinity Sliding Mode Controller Design for a Human Swing Leg System

Hazem I. Ali[1], Azhar J. Abdulridha[2*]

Authors affiliations:
1) Control and Systems Engineering Dept., University of Technology Baghdad–Iraq.
60143@uotechnology.edu.iq

2*) Control and Systems Engineering Dept., University of Technology Baghdad–Iraq.
60147@uotechnology.edu.iq

Paper History:

Received: 23th Oct. 2019

Revised: 11th Dec. 2019

Accepted: 16th March 2020

Abstract

In this paper, the H-infinity Sliding Mode Control (HSMC) is designed to produce a new dynamic output feedback controller for trajectory tracking of the nonlinear human swing leg system. The human swing leg system represents the support of human leg or the humanoid robot leg which is usually modeled as a double pendulum. The thigh and shank of a human leg is represented by two pendulum links and the hip joint will connect the upper body to the thigh and the knee joint will connect the thigh to the shank. The external torques (servo motors) are applied at the hip and knee joints to move the muscles of thigh and shank. The results show that the HSMC can robustly stabilize the system and achieve a desirable time response specification better than if only H-infinity or SMC is used. This controller achieves the following specifications: $t_s = 0.85$ *sec*, $e_{ss} = 0.01^o$ for hip joint and $t_s = 0.75$ *sec*, $e_{ss} = 0.02^o$ for knee joint.

Keywords: Human Swing Leg System, Full State Feedback Controller, H-infinity, Sliding Mode Control (SMC), Uncertain System.

تصميم مسيطرنوع H اللانهائيه ذو نمط انزلاقي لنظام الساق البشرية المتأرجحة

حازم ابراهيم علي ، ازهار جبار عبدالرضا

الخلاصة:

في هذا البحث، يتم تصميم مسيطرنوع H اللانهائيه ذو النمط الأنزلاقي لإنتاج مخرج جديد بالسيطره الراجعة وذلك لتتبع المسار للنظام اللاخطي للساق البشرية المتأرجحة. الساق البشرية المتأرجحة تعبر عن الدعامة لساق الانسان او الروبوتات البشرية و التي عادة ما تمثل كبندول مزدوج. الفخذ والساق تمثل روابط البندول من نظام الساق البشرية المتصلة ببعض عن طريق مفاصل الورك والركبة التي تربط الجزء العلوي من الجسم إلى الفخذ ثم الساق على التوالي. العزوم الإجمالية اللازمة لتحريك عضلات الفخذ والساق من قبل اثنين من العزم الخارجية (المحركات الخطوية) مطبقة على مفاصل الورك والركبة. أظهرت النتائج أن مسيطرنوع H اللانهائيه ذو النمط الإنزلاقي(HSMC) يمكن أن تحقق الإستقرارية بقوة وتحقق مواصفات زمن الاستجابة المرغوبة افضل من لو استخدم مسيطرنوع H اللانهائيه او مسيطر ذو نمط انزلاقي كلا على حده.هذا المسيطر (HSMC) حقق المحددات التاليه: زمن الاستقرار مساو ٠,٨٥ ثانية مع حاله استقرار الخطأ مساو ٠,٠١° لمفصل الورك و زمن الاستقرار مساو ٠,٧٥ ثانية مع حاله استقرار الخطأ مساو ٠,٠٢° لمفصل الركبه.

1. Introduction

The ability of human to move from one place to another is called Human movement. Walking, jogging, and running gaits are considered the parts of Human movement. Walking is one of the main gaits of movement and happens more frequently than the other ones [1]. Due to neurological injuries, such as spinal cord injury and stroke, which result in motor-incomplete gait; there are a vast number of people who lose their walking ability [2]. The swing leg system is very important; therefore, many researches have been done to control this system using different control approaches. Ono et al. [3] and Huang et al. [4], designed P controller for human swing leg system and the lost energy in joint self-impact stopper was obtained. A torque has been applied to the hip joint to restore the lost energy. Dallali et al. [5], presented a comparison between PID and Linear Quadratic Regulator (LQR) controllers. A better robustness was obtained from the LQR controller. The test was done on the robot leg from -11.5^o to 11.5^o and obtained control action about $30\ N.m$. Gregg et al. [6], implemented virtual constraints that unify the stance period, coordinate ankle and knee control on a powered prosthetic leg. To simulate the torque limit of the experimental prosthesis, the saturate prosthesis torques at $80\ N.m$. Bazargan-Lari et al. [7], proposed a nonlinear intelligent controller using Adaptive Neural Network control for human swing leg at hip and knee joints. The angular velocity for the joints was obtained

with maximum error of about 0.15% for the hip joint and 0.35% for the knee joint.
The H-infinity and Sliding Mode Control (SMC) techniques are used in the control theory to achieve stabilization and robust performance. The advantages of the H-infinity method over classical control methods which are applicable to problems with cross-coupling between channels in multivariable systems. Disadvantages of this method need a high level of mathematical understanding to apply it successfully and a reasonably good model of the system to be controlled [8]. In the SMC, the sliding surface is chosen to force the system state trajectory to move along it. The sliding surface is always chosen in such a way that led a control law guarantees to be stable [9]. SMC has been applied for uncertain systems, stochastic systems, time delay systems, and switched hybrid systems [10].
In this work, H-infinity, Sliding Mode Control and H-infinity Sliding Mode Control are the proposed controllers for the system. The main goal is to design the H-infinity Sliding Mode controller to stabilize the human swing leg system and achieve a desirable tracking.

2. System Mathematical Model

In human and humanoids, the motion of the hip and knee is achieved in the swing leg system while the ankle contribution can be neglected. The system is modeled as double pendulum with the thigh and shank represented as two links. The unconstrained double pendulum is shown in Fig.1. In this figure, the masses of thigh and shank are m_1, m_2 respectively. The lengths of thigh and shank are l_1, l_2 respectively. The hip and knee rotation angles are θ_1 and θ_2 respectively. The applied external torques are τ_1 and τ_2 to move the thigh and shank links [7, 11, 12].

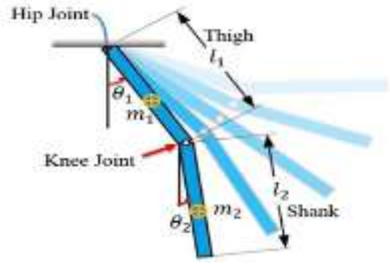

Figure (1): Schematics human swing leg [7].

The dynamic equations of the system using Lagrange's method can be represented by [7]:

$$\frac{(m_1+3\,m_2)}{3}\ l_1^2\ddot{\theta}_1+\frac{1}{2}\ m_2 l_1 l_2 \ddot{\theta}_2\ cos(\theta_1-\theta_2)+\frac{1}{2}\ m_2 l_1 l_2 \dot{\theta}_1^2\ sin(\theta_1-\theta_2)+\frac{(m_1+2\,m_2)}{2}\ g\ \ l_1\, sin\,\theta_1=\tau_1 \quad (1)$$

$$\frac{1}{3}\ m_2\ l_2^2\ddot{\theta}_2+\frac{1}{2}\ m_2 l_1 l_2 \ddot{\theta}_1\ cos(\theta_1-\theta_2)+\frac{1}{2}\ m_2 l_1 l_2 \dot{\theta}_1^2\ sin(\theta_1-\theta_2)+\frac{1}{2}\ m_2\ g\ \ l_2\, sin\,\theta_2=\tau_2 \quad (2)$$

From eq. (1) and eq. (2), $\ddot{\theta}_1$ and $\ddot{\theta}_1$are [11, 12]:

$$\ddot{\theta}_1=\frac{K_4\big(\tau_1-K_2\ \dot{\theta}_2^2\ sin(\theta_1-\theta_2)-K_3\, sin\,\theta_1\big)-K_2\, cos(\theta_1-\theta_2)\big(\tau_2+K_2\ \dot{\theta}_1^2\ sin(\theta_1-\theta_2)-K_5\, sin\,\theta_2\big)}{(K_1K_4-K_2^2\, cos(\theta_1-\theta_2)^2)} \quad (3)$$

$$\ddot{\theta}_2=\frac{K_1\ \big(\tau_2+K_2\ \dot{\theta}_1^2\ sin(\theta_1-\theta_2)-K_5\, sin\,\theta_2\big)-K_2\, cos(\theta_1-\theta_2)\big(\tau_1-K_2\ \dot{\theta}_2^2\ sin(\theta_1-\theta_2)-K_3\, sin\,\theta_1\big)}{(K_1K_4-K_2^2\, cos(\theta_1-\theta_2)^2)} \quad (4)$$

where $K_1=\frac{(m_1+4m_2)}{4}\ l_1^2$, $K_2=\frac{m_2 l_1 l_2}{2}$, $K_3=\frac{(m_1+2m_2)}{2} g\ l_1$, $K_4=\frac{m_2}{4} l_2^2$, $K_5=\frac{m_2}{2} g\ l_2$
Assume the state variables are [11]:

$x_1=\theta_1$: angular position of the upper link.
$x_2=\theta_2$: angular position of the lower link.
$x_3=\dot{\theta}_1$: angular velocity of the upper link.
$x_4=\dot{\theta}_2$: angular velocity of the lower link.
so that

$$\dot{x}_1=x_3 \quad (5)$$
$$\dot{x}_2=x_4 \quad (6)$$

$$\dot{x}_3=\frac{K_4\big(\tau_1-K_2\ x_4^2\ sin(x_1-x_2)-K_3\, sin(x_1)\big)-K_2\, cos(x_1-x_2)\big(\tau_2+K_2\ x_3^2\ sin(x_1-x_2)-K_5\, sin(x_2)\big)}{(K_1K_4-K_2^2\, cos(x_1-x_2)^2)} \quad (7)$$

$$\dot{x}_4=\frac{K_1\ \big(\tau_2+K_2\ x_3^2\ sin(x_1-x_2)-K_5\, sin(x_2)\big)-K_2\, cos(x_1-x_2)\big(\tau_1-K_2\ x_4^2\ sin(x_1-x_2)-K_3\, sin(x_1)\big)}{(K_1K_4-K_2^2\, cos(x_1-x_2)^2)} \quad (8)$$

By linearizing eq. (5) to eq. (8) using Jacobeans' method with the following initial condition: $(\theta_1,\ \theta_2)=(30^o, 10^o)$, $(\dot{\theta}_1, \dot{\theta}_2)=$ (0.3, 0.25) *rad/sec*, with$(\tau_1, \tau_2)=(0.5, 0.3)$ *N.m*, and the resulting state space representation for the system is:

$$\dot{x}(t)=Ax(t)+Bu(t) \quad (9)$$
$$y(t)=Cx(t)+Du(t) \quad (10)$$

where A, B, C and D are obtained as:

$$A=\begin{bmatrix}0 & 0 & 1 & 0\\ 0 & 0 & 0 & 1\\ -18.9615 & 2.8818 & -0.2155 & -0.1274\\ 20.2204 & -23.9035 & 0.6116 & 0.1796\end{bmatrix}, B=\begin{bmatrix}0 & 0\\ 0 & 0\\ 49.2616 & -69.4362\\ -69.4362 & 197.0466\end{bmatrix},$$
$$C=\begin{bmatrix}1 & 0 & 0 & 0\\ 0 & 1 & 0 & 0\end{bmatrix}, D=\begin{bmatrix}0 & 0\\ 0 & 0\end{bmatrix} \quad (11)$$

The parameters of human swing leg system are given in Table 1.

Table (1): The parameters of human swing leg model [7, 13].

parameter	value	unit
m_1, m_2	0.1	*kg*
l_1, l_2	0.55	*m*

Consider the system with uncertainty and external disturbance with matching condition is described as:

$$\dot{x}=(A+\Delta A)x+(B+\Delta B)u+d \quad (12)$$

where $x\in R^n$, A and $\Delta A\in R^{n\times n}$, B and $\Delta B\in R^{n\times m}$ and $u\in R^n$.The matrices ΔA and ΔB represent the uncertainties in the matrices A and B respectively and d refers to external disturbance. Assume the perturbations are about $\pm 10\%$ of system parameters *i.e.*$m_1, m_2=0.1(1\pm 10\%)$ and $l_1, l_2=0.55(1\pm$

10%). Hence, $\varDelta A$, $\varDelta B$ and d satisfy matching condition, where

$$\varDelta A = B\, A_{\delta}, \varDelta B = B\, B_{\delta} \text{ and } d = B\, \delta \qquad (13)$$

and

$$\varDelta A = \begin{bmatrix} 0 & 0 & 0 & 0 \\ 0 & 0 & 0 & 0 \\ 0.9504 & 0.5114 & 0 & 0 \\ -1.0465 & 1.3813 & 0 & 0 \end{bmatrix},$$
$$A_{\delta} = \begin{bmatrix} 0.0235 & 0.0403 & 0 & 0 \\ 0.003 & 0.0212 & 0 & 0 \end{bmatrix},$$
$$\varDelta B = \begin{bmatrix} 0 & 0 \\ 0 & 0 \\ -12.2506 & 17.2678 \\ 17.2678 & -49.0026 \end{bmatrix},$$
$$B_{\delta} = \begin{bmatrix} -0.2487 & 0 \\ 0 & -0.2487 \end{bmatrix} \qquad (14)$$

Then substituting eq. (13) in eq. (12), yields:

$$\dot{x} = A\, x + B\, u + B(A_{\delta}\, x + B_{\delta}\, u + \delta) \qquad (15)$$

The constraints on input torques and output joint angles for the system are specified as:

$$-20 \le \tau_1 \le 20, -20 \le \tau_2 \le 20,$$
$$-90^{o} \le \theta_1 \le 90^{o}, -5^{o} \le \theta_2 \le 150^{o} \qquad (16)$$

3. Controller Design

In this work, H-infinity, Sliding Mode Control and H-infinity Sliding Mode Control are proposed to control the system. The SMC is one of the effective nonlinear robust control methods which has two phases: the reaching phase and the sliding phase. In the reaching phase, a reaching control law is applied to lead the system states to be on the sliding line and the system is called to be in the sliding mode. When the system states are on the sliding line, a nominal control law is applied to lead the system states along the sliding line to the origin [11, 12, 14]. Fig.2 illustrates the reaching phase and the sliding surface in the SMC design.

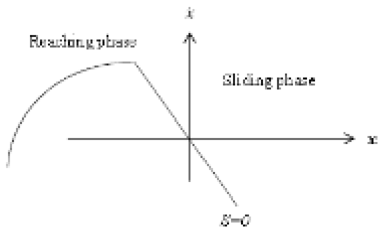

Figure (2): Two steps of SMC design.

There are two steps to design SMC; the first step is selecting the sliding surface, and the second step is designing the control input to force the system trajectory toward the sliding surface [15]. If a system has *m* inputs, there are *m* hyperplanes [16]. For the human swing leg system which has two inputs so there are two hyperplanes [11]. These hyperplanes are defined as [16]:

$$S(t) = F\, x(t) \qquad (17)$$

where F is $m \times n$ matrix which represent the gain to form sliding surface. Differentiating eq. (17) and substituting eq. (9) in the resulting equation, yields [11, 17]:

$$\dot{S} = F(Ax + Bu) \qquad (18)$$

The sliding mode control law is:

$$u = u_o + u_s \qquad (19)$$

where u_o is the nominal control and u_s is discontinuous control input if the proposed controller is Sliding Mode Control only, but u_o will be designed based on H-infinity controller if the proposed controller is H-infinity Sliding Mode Control.

The vector $S(t) = 0$ represents the intersection of all *m* sliding hyperplanes passing through the origin of the state space. The F matrix is computed by minimizing a quadratic objective function involving the state vector and the effective input, that is, by solving a linear quadratic (LQ) problem. This approach is called the Optimal Sliding Mode controller where the objective function to be minimized is [16]:

$$J = \int_0^{\infty} (x^T\, Q\, x)\, dt \qquad (20)$$

For the LQ control, it is necessary to have the input term in the quadratic objective function and the input term is not presented in the objective function in eq. (20), and the constraints are that the system is on the intersection on *m* sliding hyperplanes. The F matrix is not specified a priori and will come out as a solution to the problem. Using the similarity transformation [11, 16]:

$$q = H\, x \qquad (21)$$

where $q \in R^n$ represents the transformed state. The $H \in R^n$ represents the transformation matrix is:

$$H = [n \quad B\,]^T \qquad (22)$$

where the matrix $n \in R^{n \times (n-m)}$, the columns of this matrix are composed of basis vectors of the null space of B^{T}. Differentiating eq. (21) and substituting eq. (15) and eq. (21) in the resulting equation, yields:

$$\dot{q} = \mathcal{A}\, q + \mathcal{B}u + \Delta\mathcal{A}\, q + \Delta\mathcal{B}u + £ \qquad (23)$$

where

$$\mathcal{A} = HAH^{-1}, \Delta\mathcal{A} = HBA_{\delta}H^{-1} = \begin{bmatrix} 0 & 0 \\ \Delta\mathcal{A}_{21} & \Delta\mathcal{A}_{22} \end{bmatrix}$$
$$, \mathcal{B} = HB = \begin{bmatrix} 0 \\ \mathcal{B}_2 \end{bmatrix}, \ \Delta\mathcal{B} = HBB_{\delta} = \begin{bmatrix} 0 \\ \Delta\mathcal{B}_2 \end{bmatrix} \text{ and } £ = HB\delta = \mathcal{B}\delta \qquad (24)$$

The matrix H has a special structure, the first $(n-m)$ rows of $\mathcal{B}$ turn out to be zeroes and the vector q is decomposed as follows:

$$q = \begin{bmatrix} q_1 \\ q_2 \end{bmatrix} \qquad (25)$$

where q_1 and q_2 are $(n-m)$ and m-dimensional vectors, respectively. Partitioning eq. (23), yields:

$$\begin{bmatrix} \dot{q}_1 \\ \dot{q}_2 \end{bmatrix} = \begin{bmatrix} \mathcal{A}_{11} & \mathcal{A}_{12} \\ \mathcal{A}_{21} & \mathcal{A}_{22} \end{bmatrix} \begin{bmatrix} q_1 \\ q_2 \end{bmatrix} + \begin{bmatrix} 0 \\ \mathcal{B}_2 \end{bmatrix} u + \begin{bmatrix} 0 & 0 \\ \Delta\mathcal{A}_{21} & \Delta\mathcal{A}_{22} \end{bmatrix} \begin{bmatrix} q_1 \\ q_2 \end{bmatrix} + \begin{bmatrix} 0 \\ \Delta\mathcal{B}_2 \end{bmatrix} u + \begin{bmatrix} 0 \\ \mathcal{B}_2 \end{bmatrix} \delta \qquad (26)$$

Substituting eq. (21) in eq. (20), yields:

$$J = \int_0^{\infty} (q^T\, Q_q\, q)\, dt \qquad (27)$$

where,

$$Q_q = (H^{-1})^T\, QH^{-1} \qquad (28)$$

If $\mathrm{Q} = \mathrm{Q}^{\mathrm{T}} \ge 0$, then $\mathrm{Q_q} = \mathrm{Q_q}^{\mathrm{T}} \ge 0$; because the signs of eigenvalues are preserved under congruence transformation. Partitioning $\mathrm{Q_q}$ to form the partition of q in eq. (28) as:

$$Q_q = \begin{bmatrix} Q_r & N \\ N^T & R \end{bmatrix} \quad (29)$$

Substituting eq. (25) and eq. (29) in eq. (27), yields:

$$J = \int_0^\infty ({q_1}^T Q_r\, q_1 + 2{q_1}^T N\, q_2 + {q_2}^T R\, q_2)\, dt \quad (30)$$

The matrix Q is selected by trial and error to be:

$$Q = 10^5 \begin{bmatrix} 1 & 0 & 0 & 0 \\ 0 & 1 & 0 & 0 \\ 0 & 0 & 1 & 0 \\ 0 & 0 & 0 & 1 \end{bmatrix} \quad (31)$$

From the selected Q matrix and according to eq. (28) and eq. (29) the matrices Q_q, Q_r, R and N are obtained as follows:

$$Q_q = 10^5 \begin{bmatrix} 1 & 0 & 0 & 0 \\ 0 & 1 & 0 & 0 \\ 0 & 0 & 0.0018 & 0.0007 \\ 0 & 0 & 0.0007 & 0.0003 \end{bmatrix},$$

$$Q_r = 10^5 \begin{bmatrix} 1 & 0 \\ 0 & 1 \end{bmatrix},$$

$$R = \begin{bmatrix} 182.9 & 71.7 \\ 71.7 & 30.4 \end{bmatrix}, N = \begin{bmatrix} 0 & 0 \\ 0 & 0 \end{bmatrix} \quad (32)$$

for $S = 0$, the $(n-m)$ dimensional dynamics is represented by [16]:

$$\dot{q}_1 = \mathcal{A}_{11}\, q_1 + \mathcal{A}_{12} q_1 \quad (33)$$

Then sliding hyperplanes can be described as

$$S = K\, q_1 + q_2 \quad (34)$$

where the gain matrix K is obtained for the minimum value of J is:

$$K = R^{-1} ({\mathcal{A}_{12}}^T P_s + N^T) \quad (35)$$

where P_s matrix is found by the solution of the Riccati equation:

$$P_s(\mathcal{A}_{11} - \mathcal{A}_{12} R^{-1} N^T) + (\mathcal{A}_{11} - \mathcal{A}_{12} R^{-1} N^T)^T P_s - P_s \mathcal{A}_{12} R^{-1} {\mathcal{A}_{12}}^T P_s + Q_q - N R^{-1} N^T = 0 \quad (36)$$

where

$$P_s = \begin{bmatrix} 10 & 0 \\ 0 & 10 \end{bmatrix} \quad (37)$$

The gain matrix K becomes:

$$K = \begin{bmatrix} 0.2813 & 0.8035 \\ -1.2053 & -1.7065 \end{bmatrix} \quad (38)$$

From eq. (17) and eq. (34), F matrix is:

$$F = [K \quad I_m]H, = \begin{bmatrix} 0.4926 & -0.6944 & 0.4926 & -0.6944 \\ -0.6944 & 1.9705 & -0.6944 & 1.9705 \end{bmatrix} \quad (39)$$

The selection of matrix F or matrix K is to ensure the system stability on the intersection of all hyperplanes. The standard LQ problem provided $R > 0$ and if Q is selected to be positive definite, R will be positive definite [16].

In SMC, u_o is conducted to satisfy the desired specification for nominal system corresponds to $\dot{S}$=0, from eq. (18), eq. (19) becomes:

$$u_o = -(FB)^{-1} FA\, x \quad (40)$$

The uncertain parameters in human swing leg system are represented as a structured parametric uncertainty. This problem can be defined by the configuration in Fig.3. The G is the plant and $d(t)$ is the disturbance, whose effect on the output signal to be minimize. The input $u_o(t)$ is the control signal which used to achieve this goal. The output $e(t)$ represents the signal to be minimized and the output $y(t)$ represents the system states which are available for feedback [17-19].

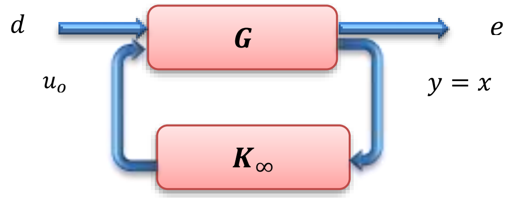

Figure (3): A full state feedback H-infinity control structure.

Therefore, the full state feedback H-infinity controller will be expressed as [8, 16]:

$$\dot{x} = Ax + B\, u_o + Bd \quad (41)$$

$$e = C_1 x + D_1 u_o \quad (42)$$

$$y = x \quad (43)$$

where $d = (A_\delta\, x + B_\delta\, u_o + \delta)$ is the disturbance matrix, and C_1, D_1 represent the controller design matrix. The solution of the corresponding H-infinity problem based on Riccati equation requires the following assumptions to be satisfied [8, 16]:

- (A, B) is stabilizable, (C_1, A) is detectable.
- $C_1^T\, D_1 = 0$ and $D_1^T\, D_1 = I$.

The H-infinity norm of the closed-loop transfer function between error and disturbance (T_{ed}) should be less than a given value of γ as:

$$\| T_{ed}(s) \|_\infty < \gamma \quad (44)$$

d tries to maximize the cost function Jwhile the control signal $u_o$tries to minimize it. The physical meaning of the relation given above competes to each other within infimum (inf) and supremum (sup). This problem of $inf - sup$ optimization can be written as [16]:

$$\inf_{u_o} \sup_{d} J(u_o, d) < \infty \quad (45)$$

and

$$J(e, d) = \int_0^\infty (e^T e - \gamma^2 d^T d) dt \quad (46)$$

assume that d and $u_o$have the following structures:

$$d = K_d\, x \quad (47)$$

and

$$u_o = -K_\infty\, x \quad (48)$$

where K_d and K_∞ represent the feedback gains for disturbance and controller. Substituting eq. (47) and eq. (48) in eq. (42), yields:

$$e = (C_1 - D_{11} K_\infty)\, x \quad (49)$$

therefore

$$e^T e = x^T (C_1^T C_1 + K_\infty^T K_\infty)\, x \quad (50)$$

and

$$d^T d = (K_d\, x)^T (K_d\, x) = x^T (K_d^T K_d)\, x \quad (51)$$

Substituting eq. (50) and eq. (51) in eq. (45), gives:

$$J(u_o, d) = \int_0^\infty x^T (C_1^T C_1 + K_\infty^T K_\infty - \gamma^2 K_d^T K_d) x\, dt \quad (52)$$

and substituting eq. (47) and eq. (48) in eq. (41), yields:

$$\dot{x} = (A - BK_\infty + BK_d)x \quad (53)$$

where

$$K_\infty = B^T P_1, K_d = \frac{1}{\gamma^2} B^T P_1 \quad (54)$$

The Riccati equation required to solve this optimal problem is:

$$P_1 A + A^T P_1 + Q_1 - P_1 B \left(I - \frac{1}{\gamma^2}\right) B^T P_1 = 0 \quad (55)$$

where P_1 is a positive semi-definite symmetric matrix , and $Q_1 = C_1^T C_1$. By trial and error Q_1 matrix is selected as:

$$Q_1 = \begin{bmatrix} 400 & 0 & 0 & 0 \\ 0 & 300 & 0 & 0 \\ 0 & 0 & 10 & 0 \\ 0 & 0 & 0 & 10 \end{bmatrix},$$

$$C_1 = \begin{bmatrix} 20 & 0 & 0 & 0 \\ 0 & 17.3205 & 0 & 0 \\ 0 & 0 & 3.1633 & 0 \\ 0 & 0 & 0 & 3.1633 \end{bmatrix} \quad (56)$$

The values of P_1, K_c and K_d of the system are:

$$P_1 = \begin{bmatrix} 71.1377 & 2.3911 & 1.3238 & 0.4643 \\ 2.3911 & 56.3147 & 0.3972 & 0.2880 \\ 1.3238 & 0.3972 & 0.2491 & 0.0888 \\ 0.4643 & 0.2880 & 0.0888 & 0.0596 \end{bmatrix},$$

$$K_\infty = \begin{bmatrix} 32.9699 & -0.4319 & 6.1050 & 0.2348 \\ -0.4211 & 29.1696 & 0.1993 & 5.5801 \end{bmatrix},$$

$$K_d = \begin{bmatrix} 21.7925 & -0.2855 & 4.0353 & 0.1552 \\ -0.2784 & 19.2806 & 0.1318 & 3.6883 \end{bmatrix} \quad (57)$$

By trial and error γ is selected to be:

$$\gamma = 1.23 \quad (58)$$

To compute the discontinue controller, eq. (48) is substituted in eq. (15) to give:

$$\dot{x} = (A - BK_\infty)x + Bu_s + B\{(A_\delta - B_\delta K_\infty) x + B_\delta u_s + \delta\} \quad (59)$$

In the reaching phase, assuming that the closed-loop system has no finite-escape time, the switching surface is guarantee reached in finite time by control law despite the disturbance or uncertainty. The sliding motion is completely independent of the uncertainty [20]. For human swing leg system, the suitable u_s is represented as a unit control signal. This leads to what is called **"unity sliding mode control"**. For HSMC, u_s is

$$u_s = -\sigma(\|x\|) \frac{B^T \nabla V}{\|B^T \nabla V\|} \quad (60)$$

for SMC, u_s is:

$$u_s = -(FB)^{-1} \sigma_{SMC}(\|x\|) \frac{B^T \nabla V}{\|B^T \nabla V\|} \quad (61)$$

The Lyapunov function with a positive definite matrix P is:

$$V = x^T Px = S^T S = x^T F^T Fx \quad (62)$$

where $P = F^T F$, differentiating V with respect to time, such that $\dot{V} < 0, \forall x \neq 0$:

$$\dot{V} = \nabla V^T \dot{x} = 2S^T \dot{S} = 2x^T F^T F \dot{x} \quad (63)$$

where $\nabla V^T = 2x^T F^T F = 2x^T P$, then substituting eq. (٥٩) in eq. (6٣), yields:

$$\dot{V} = \nabla V^T (A - BK_\infty)x + \nabla V^T B\, u_s + \nabla V^T B\big((A_\delta - B_\delta K_\infty)x + B_\delta u_s + \delta\big) \quad (64)$$

where

$$\nabla V^T (A - BK_\infty)x = 2x^T P(A - BK_\infty)x = -x^T Q_{HSMC} x \leq 0 \quad (65)$$

where

$$P = \begin{bmatrix} 0.7248 & -1.7103 & 0.7248 & -1.7103 \\ -1.7103 & 4.3649 & -1.7103 & 4.3649 \\ 0.7248 & -1.7103 & 0.7248 & -1.7103 \\ -1.7103 & 4.3649 & -1.7103 & 4.3649 \end{bmatrix},$$

$$Q_{HSMC} = 10^4 \begin{bmatrix} 1.0608 & -2.2816 & 0.1733 & 0.4246 \\ -2.6606 & 5.7658 & -0.4342 & 1.0731 \\ 1.0608 & -2.2816 & 0.1733 & -1.4246 \\ -2.6606 & 5.7658 & -0.4342 & 1.0731 \end{bmatrix}$$

(66)

the A_δ , B_δ and δ are bounded, so

$$\|(A_\delta - B_\delta K_\infty)\| \leq \alpha, \| B_\delta \| \leq \beta, \|\delta\| \leq \varepsilon \quad (67)$$

and

$$\|(A_\delta - B_\delta K_\infty)x + B_\delta u_s + \delta\| \leq \alpha\|x\| + \beta\sigma(\|x\|) + \varepsilon$$

(68)

where α, β and ε are positive constant, substituting eq. (65), eq. (67) and eq. (68) in eq. (64), yields:

$$\dot{V} \leq -x^T Q_{HSMC} x - \sigma(\|x\|)\|B^T \nabla V\| + \|B^T \nabla V\|\{\alpha\|x\| + \beta\sigma(\|x\|) + \varepsilon\} \leq -\|B^T \nabla V\|\{\sigma(\|x\|)(1 - \beta) - \alpha\|x\| - \varepsilon\} \leq 0 \quad (69)$$

where $\{\sigma(\|x\|)(1 - \beta) - \alpha\|x\| - \varepsilon\} \geq 0$, so that

$$\sigma(\|x\|) = \frac{1}{1-\beta}\{\alpha\|x\| + k + \varepsilon\} \quad (70)$$

where $k > 0$ is scalar gain to replace the inequality from control equation.

Let $k = 0.1$, so that $\alpha = 8.3988, \beta = 0.2487, \varepsilon = 0.1414, \sigma(\|x\|) = 5.75$ (71)

For SMC, to compute the discontinues controller, eq. (65) becomes:

$$\dot{V} = \nabla V^T\{(A - B(FB)^{-1}FA)x + B\, u_s + B\big((A_\delta - B_\delta(FB)^{-1}FA)x + B_\delta u_s + \delta\big)\} = \nabla V^T(A - B(FB)^{-1}FA)x + \nabla V^T B\, u_s + \nabla V^T B\big((A_\delta - B_\delta(FB)^{-1}FA)x + B_\delta u_s + \delta\big) \quad (72)$$

Let

$$\nabla V^T(A - B(FB)^{-1}FA)x = 2x^T P(A - B(FB)^{-1}FA) = -x^T Q_{SMC} x \leq 0 \quad (73)$$

where $Q_{SMC} = 2P(A - B(FB)^{-1}FA)$ equals to:

$$Q_{SMC} = \begin{bmatrix} 0.0931 & -0.0703 & 0.0007 & 0.0016 \\ -0.2267 & 0.1800 & -0.0026 & -0.0044 \\ 0.0931 & -0.0703 & 0.0009 & 0.0016 \\ -0.2267 & 0.1800 & -0.0026 & -0.0026 \end{bmatrix}$$

(74)

A_δ , B_δ and δ are bounded as:

$$\|(A_\delta - B_\delta(FB)^{-1}FA)\| \leq \alpha_{SMC}, \| B_\delta \| \leq \beta, \|\delta\| \leq \varepsilon \quad (75)$$

and

$$\|(A_\delta - B_\delta(FB)^{-1}FA)x + B_\delta u_s + \delta\| \leq \alpha_{SMC}\|x\| + \beta\sigma_{SMC}(\|x\|) + \varepsilon \quad (76)$$

where α_{SMC}, β and ε are positive constants and $\|u_s\| \leq \sigma_{SMC}(\|x\|)$.

Substituting eq. (73), eq. (75) and eq. (76) in eq. (72), yields:

$$\dot{V} \le -x^T Q_{SMC} x - \sigma_{SMC}(\|x\|)\|B^T \nabla V\| + \|B^T \nabla V\|\{\alpha_{SMC}\|x\| + \beta\sigma_{SMC}(\|x\|) + \varepsilon\} \le -\|B^T \nabla V\|\{\sigma_{SMC}(\|x\|)(1-\beta) - \alpha_{SMC}\|x\| - \varepsilon\} \le 0 \quad (77)$$

the $\{\sigma_{SMC}(\|x\|)(1-\beta) - \alpha_{SMC}\|x\| - \varepsilon\} \ge 0$, so that

$$\sigma_{SMC}(\|x\|) = \frac{1}{1-\beta}\{\alpha_{SMC}\|x\| + k + \varepsilon\} \quad (78)$$

Let $k = 0.1$, and then $\alpha_{SMC} = 18.675$, $\beta = 0.2487$, $\varepsilon = 0.1414$, $\sigma_{SMC}(\|x\|) = 50.72$, $(FB)^{-1}\sigma_{SMC}(\|x\|) = \begin{bmatrix} 0.0928 & 0.0363 \\ 0.0363 & 0.0154 \end{bmatrix}$
so that

$$\dot{V} \le -k\|B^T \nabla V\|, \forall \|x\| \ne 0 \quad (79)$$

Eq. (79) implies that in a finite time, the trajectory reaches the sliding surface and remains on the sliding surface for all future time. Note that the reaching time is related to the magnitude of the gain $\sigma_{SMC}(\|x\|)$ for SMC or $\sigma(\|x\|)$ for HSMC directly, and the unit vector term $\frac{B^T \nabla V}{\|B^T \nabla V\|}$ of the control law is effective on the finite reaching time [15, 20]. The SMC law for the system dynamics in eq. (19) is:

$$u = -(FB)^{-1}\{FA\,x + \sigma_{SMC}(\|x\|)\frac{B^T \nabla V}{\|B^T \nabla V\|}\} \quad (80)$$

and for HSMC is:

$$u = -K_\infty\, x - \sigma(\|x\|)\frac{B^T \nabla V}{\|B^T \nabla V\|} \quad (81)$$

The SMC has chattering problem, which is a very high frequency oscillation of the sliding variable around the sliding manifold. The chattering is undesirable for the real systems and actuator. Many approaches have been projected to overcome the chattering phenomenon. In this work, to eliminate the chattering phenomena a small positive value (μ) is added to denominator of the unit vector to approximate the discontinuous controller u_s as [20]:

$$\frac{B^T \nabla V}{\|B^T \nabla V\|} \approx \frac{B^T \nabla V}{\|B^T \nabla V\| + \mu} \quad (82)$$

where μ is a positive value. For $S \ne 0$, it can be observed that point wise, when μ approaches to 0 then:

$$\lim_{\mu \to 0} \frac{B^T \nabla V}{\|B^T \nabla V\| + \mu} = \frac{B^T \nabla V}{\|B^T \nabla V\|} \quad (83)$$

The control law for SMC becomes

$$u = u_o - (FB)^{-1}\sigma_{SMC}(\|x\|)\frac{B^T \nabla V}{\|B^T \nabla V\| + \mu} \quad (84)$$

and the control law for HSMC becomes

$$u = u_o - \sigma_{HSMC}(\|x\|)\frac{B^T \nabla V}{\|B^T \nabla V\| + \mu} \quad (85)$$

In this work, the suitable value of μ is selected by trial and error to be 0.2 for the full state feedback SMC and 0.1 for the full state feedback HSMC. These selected values for both controllers made the sliding surface and control action very smooth trajectories.

4. Results and Discussion

Fig.4 illustrate the behavior of the human swing leg system without controller and the system's eigenvalues are $\{0.0463 \pm 5.4358i$, $-0.0643 \pm 3.6555i\}$. It means that the system is unstable because it has roots in the right hand side of *s*-plane. That is, the design of a suitable controller to stabilize the system and achieve the desirable specifications is required.

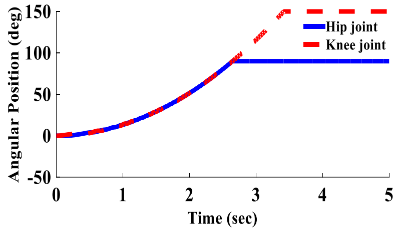

Figure (4): Time response of human swing leg system for hip and knee joints.

A comparison among the three designed controllers to specify the best robust controller for the system depending on the time response specifications, the coupling effect the control action, and the robustness is presented.

Fig.5 shows the tracking case of the nonlinear human swing leg system with H-infinity controller by the Simulink MATLAB program.

Fig.6 represents the Simulink diagram in MATLAB for the nonlinear human swing leg system which can use it for full state feedback SMC and HSMC controller with necessary modification.

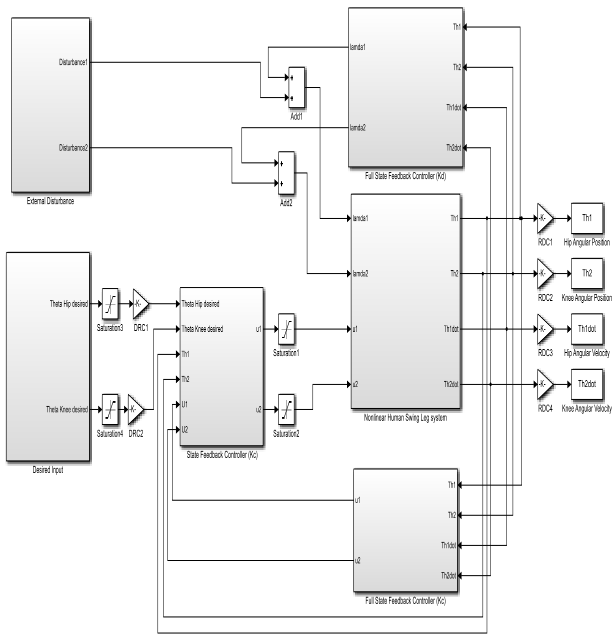

Figure (5): Simulink diagram of the nonlinear human swing leg system with H-infinity controller.

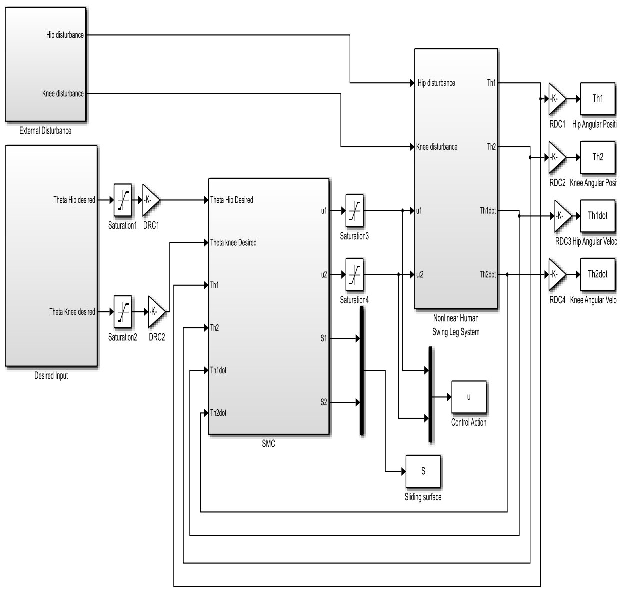

Figure (6): Simulink diagram of for the nonlinear human swing leg system SMC or HSMC controller.

Fig.7 represents the time response of angular position and control actions for hip and knee joints for the system using the three proposed controllers with initial conditions $\{30^o, 10^o, (0.3, 0.25)\ rad/sec\}$. The state trajectories obtained using HSMC approaches the equilibrium state faster than using H-infinity or SMC approaches. Also, HSMC has given better performance rather than if only one of them is used with Low control effort.

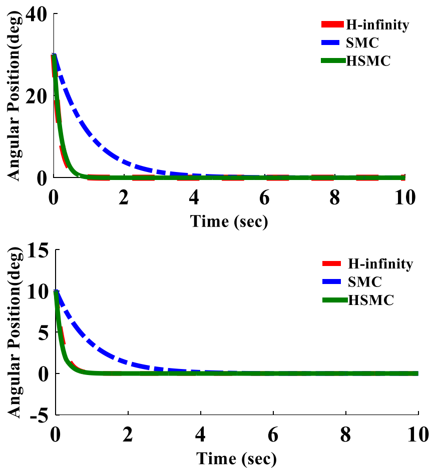

(a) angular position for hip and knee respectively.

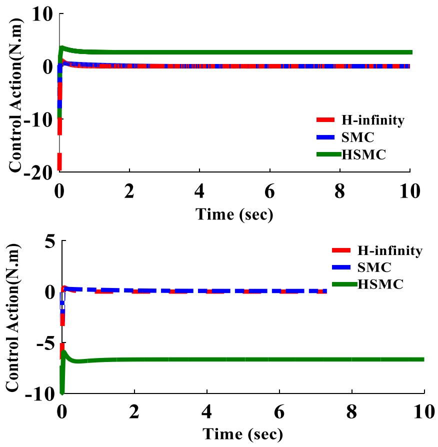

(b) control action for hip and knee respectively.

Figure (7): The states trajectories of the nonlinear human swing leg system using H-infinity controller, SMC and HSMC.

For tracking, assume the desired trajectory that the system will be follow is described as:

$$\theta_{hip\ desired} = 4\,sin\,0.5t + 3\,sin\,t + sin\,1.5t + 20,$$
$$\theta_{knee\ desired} = 0.5 \times \theta_{hip\ desired} \qquad (86)$$

Fig.8 represents the time response of angular positions and control actions for hip and knee joints of the system using the three proposed controllers for specific trajectory. It can be noticed that HSMC is better and faster to follow the desired trajectory than H-infinity or SMC controller with Low control effort.

.

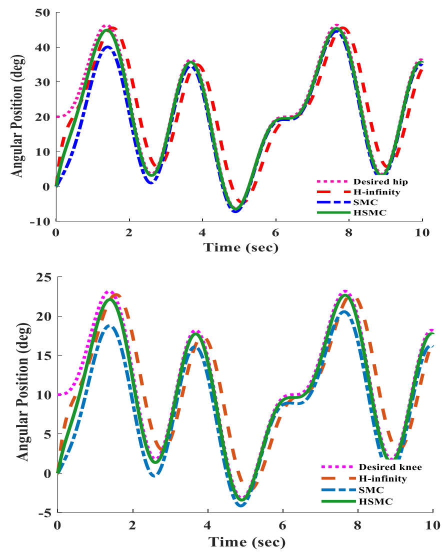

(a) angular position for hip and knee respectively.

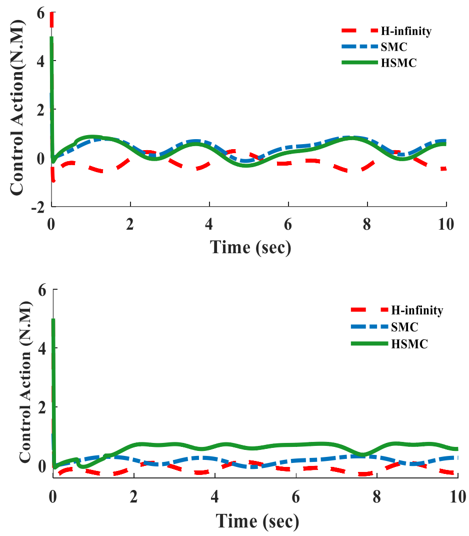

(b) control action for hip and knee respectively.

Figure (8): Tracking properties for the nonlinear human swing leg system using H-infinity controller, SMC and HSMC.

Fig.9 represents states trajectories of nonlinear system when applying external disturbance for hip and knee joints to show the ability of the three proposed controllers to overcome external disturbance. The disturbance signal which applied on the system is about 10% from the desired trajectory and it will be applied at specific time period (*i.e.* t_{low}, t_{high}). The disturbance equation describes as:

$$\theta_{\,hip\ disturbance} = \begin{cases} 0 & 0 \le t < t_{low} \\ 0.4\,sin\,0.5t + 0.3\,sin\,t + 0.1\,sin\,1.5t + 2 & t_{low} \le t \le t_{high} \\ 0 & t > t_{high} \end{cases},$$

$$\theta_{\,knee\ disturbance} = 0.5 \times \theta_{\,hip\ disturbance} \qquad (87)$$

It is noticed that SMC and HSMC can overcome the external disturbance better than H-infinity with Low control effort.

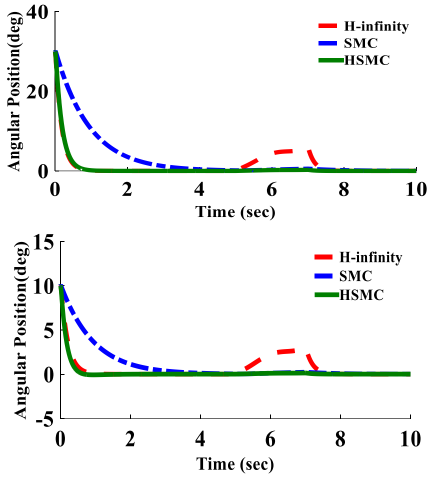

(a) angular position for hip and knee respectively.

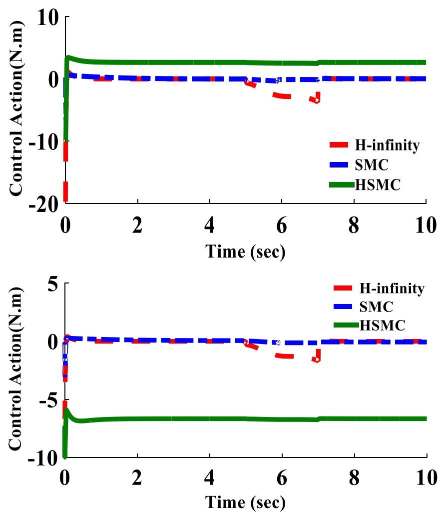

(b) control action for hip and knee respectively.

Figure (9): Disturbance rejection proprieties on state trajectories of the nonlinear human swing leg system using H-infinity controller, SMC and HSMC.

Fig.10 shows the system position trajectories of the system with a perturbation of $\pm 10\%$ in parameters of the system. It is apparent that the full state feedback H-infinity controller and SMC can effectively compensate the system parameters perturbation without eliminating the steady state error. The HSMC can effectively compensate the system parameters perturbation and achieve the required robustness for the system with a desirable time response better than H-infinity and SMC when used separately.

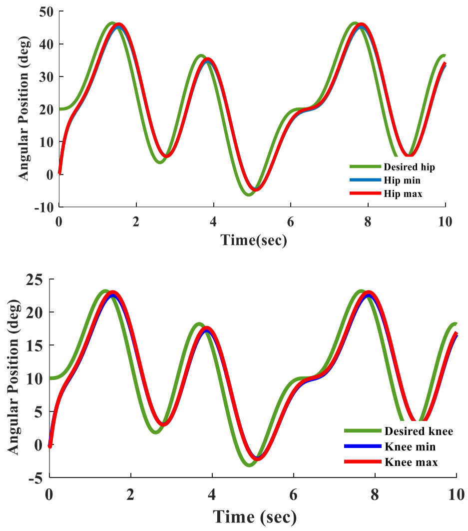

(a) H-infinity for hip and knee position respectively.

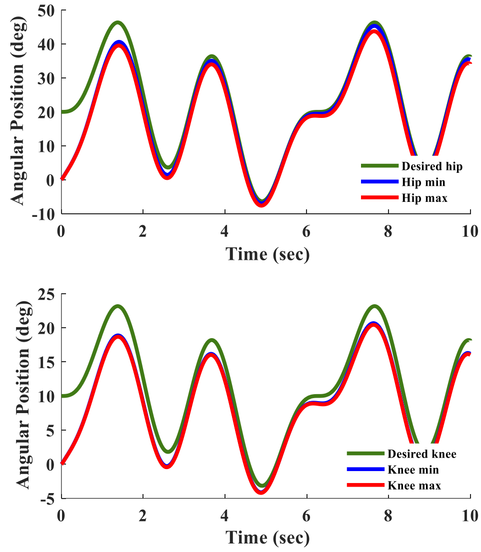

(b) SMC for hip and knee position respectively.

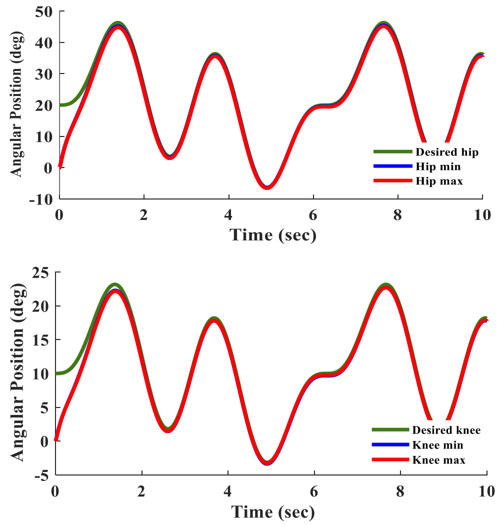

(c) HSMC for hip and knee position respectively.

Figure (10): Time response of the nonlinear system with $\pm 10\%$ perturbation in system parameters.

Fig.11 represents the states trajectories of nonlinear system when applying step inputs for hip and knee joints to show the ability of the three proposed controllers to overcome the cross coupling problem. It is noticed that H-infinity and HSMC can overcome this problem better than SMC. The trajectories of state using HSMC approaches to the steady state faster than the trajectories of state obtained using H-infinity or SMC approaches.

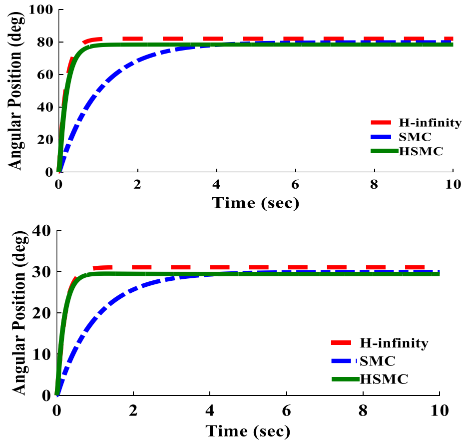

(a) the desired hip at 80^{o} and the desired knee at 30^{o}.

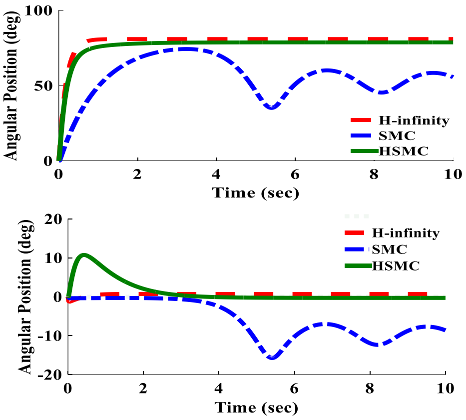

(b) the desired hip at 80^{o} and the desired knee at 0^{o}.

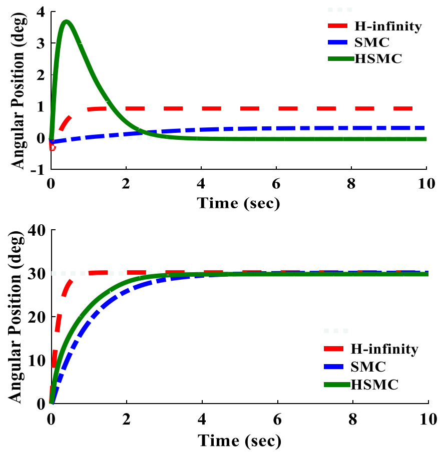

(c) the desired hip at 0^{o} and the desired knee at 30^{o}.

Figure (11): The cross coupling properties of the nonlinear human swing leg system using H-infinity controller, SMC and HSMC.

From Fig.9 can noticed that, under effect of H-infinity controller, the settling time $t_s = 1.1$ *sec* with steady state error $e_{ss} = -0.32^{o}$ for hip joint and $t_s = 1.3$ *sec* with $e_{ss} = -0.24^{o}$ for knee joint. In SMC, the $t_s = 3.3$ *sec* with $e_{ss} = 0.02^{o}$ for hip joint and $t_s = 3.1$ *sec* with $e_{ss} = 0.04^{o}$ for knee joint. In HSMC, the $t_s = 0.85$ *sec* with $e_{ss} = 0.01^{o}$ for hip joint and $t_s = 0.75$ *sec* with $e_{ss} = 0.02^{o}$ for knee joint. So that, HSMC has given better performance than if only one of them is used.

5. Conclusions

In this paper, H-infinity, SMC and HSMC were proposed to achieve trajectory tracking and stabilization of the uncertain and nonlinear human swing leg system. The results showed that the effectiveness and the applicability of the proposed controller. The design of the robust control using H-infinity and SMC for this nonlinear and uncertain systems was necessary. Although the H-infinity controller improves the transient response of the system and compensates the cross coupling effect, there was still error. The SMC can effectively attenuates the error but the resulting transient response was not desirable in addition to the high effect of the cross coupling. The design using the HSMC was very efficient and it has given a response better than if only one of them was used. The superiority of the HSMC was because it can achieve the design requirements that arise from both H-infinity and SMC simultaneously.

References

[1] Bazargan-Lari Y., Eghtesad M., Khoogar A. R. and Mohammad-Zadeh A. (2015), Tracking Control of a Human Swing Leg Considering Self-Impact Joint Constraint by Feedback Linearization Method, Control Engineering and Applied Informatics (CEAI), Vol. 17, No. 1, pp. 99-110.

[2] Mokhtarian A., Fattah A. and Agrawal S. K. (2014), A Passive Swing-Assistive Planar External Orthosis for Gait Training on Treadmill, The Brazilian Society of Mechanical Sciences and Engineering.

[3] Ono K., Furuichi T. and Takahashi R. (2004), Self-Excited Walking of a Biped Mechanism with Feet, The International Journal of Robotics Research, Vol. 23, No. 1, pp. 55-68.

[4] Huang Q., Hase T., and Ono K. (2007), Passive/Active Unified Dynamic Walking for Biped Locomotion, In Robotics and Biomimetic, ROBIO 2007. IEEE International Conference, pp. 964-971.

[5] Dallali H., Medrano-Cerda G. A. and Brown M. (2010), A Comparison of Multivariable and Decentralized Control Strategies for Robust Humanoid Walking, UKACC International Conference on CONTROL 2010, pp. 235 – 240.

[6] Gregg R. D., Lenzi T., Hargrove L. J. and Sensinger J. W. (2014), Virtual Constraint Control of a Powered Prosthetic Leg from Simulation to Experiments with Transfemoral Amputees, USAMRAA Grant, IEEE Transactions on Robotics, a publication of the IEEE Robotics and Automation Society, Vol. 30, No. 6, pp. 1455-1471.

[7] Bazargan-Lari Y., Eghtesad M., Khoogar A. R. and Mohammad-Zadeh A. (2015), Adaptive

Neural Network Control of a Human Swing Leg as a Double-Pendulum Considering Self-Impact Joint Constraint, Transactions of the Canadian Society for Mechanical Engineering, Vol. 39, No. 2, pp. 201-219.

[8] Cubillos X. C. and de Souza L. C. G. (2009), Using of H-Infinity Control Method in Attitude Control System of Rigid-Flexible Satellite, Hindawi Publishing Corporation Mathematical Problems in Engineering, Vol. 2009.

[9] Singla M., Shieh L., Song G., Xie L. and Zhang Y. (2013), A New Optimal Sliding Mode Controller Design Using Scalar Sign Function, ISA Transactions, Elsevier Ltd.

[10] Wu L., Shi P. and Gao H. (2010), State Estimation and Sliding-Mode Control of Markovian Jump Singular Systems, IEEE Transactions on Automatic Control, Vol. 55, No. 5, pp. 1213-1219.

[11] Hazem I. A.and Azhar J. A. (2018), State Feedback Sliding Mode Controller Design for Human Swing Leg System, Al-Nahrain Journal for Engineering Sciences (NJES), Vol. 21, No. 1, pp. 51-59.

[12] Hazem I. A. and Azhar J. A. (2018), H-infinity Based Full State Feedback Controller Design for Human Swing Leg, Engineering and Technology Journal, Vol. 36, Part A, No. 3, pp. 350-357.

[13] Bazargan-Lari Y., Gholipour A., Eghtesad M., Nouri M. and Sayadkooh A. (2011), Dynamics and Control of Locomotion of One Leg Walking as Self-Impact Double Pendulum, International Conference on Control, Instrumentation and Automation (ICCIA), No. 2, pp. 201-206.

[14] Zhang X., Sun L., Zhao K. and Sun L. (2013), Nonlinear Speed Control for PMSM System Using Sliding Mode Control and Disturbance Compensation Techniques, IEEE Transactions on Power Electronic, Vol. 28, No. 3, pp. 1358-1365.

[15] Raafat S. M., Al-Samarraie S. A., Mahmood A. M. (2015), Unity Sliding Mode Controller Design for Active Magnetic Bearings System, Journal of Engineering, Vol. 21, No. 6, pp. 90-106.

[16] Sinha A. (2007), Linear Systems Optimal and Robust Control, CRC Press is an imprint of Taylor and Francis Group, an Informa business.

[17] Agrachev A. A. , Morse A. S. , Sontag E. D., Sussmann H.J. and Utkin V. I., (2004), "Nonlinear and Optimal Control Theory", Cetraro, Italy.

[18] Jeong D., Kang T., Dharmayanda H., and Budiyono A. (2012), H-Infinity Attitude Control System Design for a Small-Scale Autonomous Helicopter with Nonlinear Dynamics and Uncertainties, Journal of Aerospace Engineering, Vol. 25, No. 4, Brunel University, London, pp. 501–518.

[19] Nair S. S. (2011), Automatic Weight Selection Algorithm for Designing H-Infinity Controller for Active Magnetic Bearing, International Journal of Engineering Science and Technology (IJEST), Coimbatore, India, Vol. 3, No. 1, pp. 122- 138.

[20] Shtessel Y., Edwards C., Fridman L., Levant A. (2014), Sliding Mode Control and Observation, Springer Science and Business Media (birkhauser), New York.